2.4.6 Beam polarization

2.4.6 1 Spin polarization – an overview

Before describing concepts for attaining electron and positron spin polarization for eRHIC we present a brief overview of the theory and phenomenology. We can then draw on this later as required. This overview is necessarily brief but more details can be found in [1, 2].

Self polarization

The spin polarization of an ensemble of spin–1/2 fermions with the same energies traveling in the same direction is defined as

$$\vec{P} = \langle \frac{2}{\hbar} \vec{\sigma} \rangle \qquad (1)$$

where $\vec{\sigma}$ is the spin operator in the center of mass and $\langle \ \rangle$ denotes the expectation value for the mixed spin state. We denote the single particle center–of–mass expectation value of $\frac{2}{\hbar}\vec{\sigma}$ by $\vec{S}$ and we call this the "spin". The polarization is then the average of $\vec{S}$ over an ensemble of particles such as that of a bunch of particles.

Relativistic $e^{\pm}$ circulating in the (vertical) guide field of a storage ring emit synchrotron radiation and a tiny fraction of the photons can cause spin flip from up to down and vice versa. However, the up–to–down and down–to–up rates differ, with the result that in ideal circumstances the electron (positron) beam can become spin polarized anti–parallel (parallel) to the field, reaching a maximum polarization, P_{st}, of $\frac{8}{5\sqrt{3}} = 92.4\%$. This, the Sokolov–Ternov (S–T) polarizing process, is very slow on the time scale of other dynamical phenomena occurring in storage rings, and the inverse time constant for the exponential build up is [3]:

$$\tau_{\text{st}}^{-1} = \frac{5\sqrt{3}}{8} \frac{r_{\text{e}} \gamma^5 \hbar}{m_{\text{e}} |\rho|^3} \qquad (2)$$

where r_{e} is the classical electron radius, γ is the Lorentz factor, ρ is the radius of curvature in the magnets and the other symbols have their usual meanings. The time constant is usually in the range of a few minutes to a few hours.

However, even without radiative spin flip, the spins are not stationary but precess in the external fields. In particular, the motion of $\vec{S}$ for a relativistic charged particle traveling

in electric and magnetic fields is governed by the Thomas–BMT equation $d\vec{S}/ds = \vec{\Omega} \times \vec{S}$ where s is the distance around the ring [2, 4]. The vector $\vec{\Omega}$ depends on the electric ($\vec{E}$) and magnetic ($\vec{B}$) fields, the energy and the velocity ($\vec{v}$) which evolves according to the Lorentz equation:

$$\vec{\Omega} = \frac{e}{m_{\mathrm{e}}c}\left[-\left(\frac{1}{\gamma}+a\right)\vec{B} + \frac{a\gamma}{1+\gamma}\frac{1}{c^2}(\vec{v}\cdot\vec{B})\vec{v} + \frac{1}{c^2}\left(a+\frac{1}{1+\gamma}\right)(\vec{v}\times\vec{E})\right] \tag{3}$$

$$= \frac{e}{m_{\mathrm{e}}c}\left[-\left(\frac{1}{\gamma}+a\right)\vec{B}_{\perp} - \frac{g}{2\gamma}\vec{B}_{\|} + \frac{1}{c^2}\left(a+\frac{1}{1+\gamma}\right)(\vec{v}\times\vec{E})\right] . \tag{4}$$

Thus $\vec{\Omega}$ depends on s and on the position of the particle $u \equiv (x, p_x, y, p_y, l, \delta)$ in the 6–D phase space of the motion. The coordinate δ is the fractional deviation of the energy from the energy of a synchronous particle ("the beam energy") and l is the distance from the center of the bunch. The coordinates x and y are the horizontal and vertical positions of the particle relative to the reference trajectory and $p_x = x', p_y = y'$ (except in solenoids) are their conjugate momenta. The quantity g is the appropriate gyromagnetic factor and $a = (g-2)/2$ is the gyromagnetic anomaly. For $e^{\pm}$, $a \approx 0.0011596$. $\vec{B}_{\|}$ and $\vec{B}_{\perp}$ are the magnetic fields parallel and perpendicular to the velocity.

In a simplified picture the majority of the photons in the synchrotron radiation do not cause spin flip but tend instead to randomize the $e^{\pm}$ orbital motion in the (inhomogeneous) magnetic fields. Then, if the ring is insufficiently well geometrically aligned and/or if it contains special magnet systems like the "spin rotators" needed to produce longitudinal polarization at a detector (see below), the spin–orbit coupling embodied in the Thomas–BMT equation can cause spin diffusion, i.e. depolarization. Compared to the S–T polarizing effect the depolarization tends to rise very strongly with beam energy. The equilibrium polarization is then less than 92.4% and will depend on the relative strengths of the polarization and depolarization processes. As we shall see later, even without depolarization certain dipole layouts can reduce the equilibrium polarization to below 92.4 %.

Analytical estimates of the attainable equilibrium polarization are best based on the Derbenev–Kondratenko (D–K) formalism [5, 6]. This implicitly asserts that the value of the equilibrium polarization in an $e^{\pm}$ storage ring is the same at all points in phase space and is given by

$$P_{\mathrm{dk}} = \mp\frac{8}{5\sqrt{3}}\frac{\oint ds \left\langle \frac{1}{|\rho(s)|^3}\hat{b}\cdot(\hat{n} - \frac{\partial\hat{n}}{\partial\delta})\right\rangle_s}{\oint ds \left\langle \frac{1}{|\rho(s)|^3}(1 - \frac{2}{9}(\hat{n}\cdot\hat{s})^2 + \frac{11}{18}\left(\frac{\partial\hat{n}}{\partial\delta}\right)^2)\right\rangle_s} \tag{5}$$

where $< >_s$ denotes an average over phase space at azimuth s, $\hat{s}$ is the direction of motion and $\hat{b} = (\hat{s}\times\dot{\hat{s}})/|\dot{\hat{s}}|$. $\hat{b}$ is the magnetic field direction if the electric field vanishes and the motion is perpendicular to the magnetic field. $\hat{n}$ is a unit 3–vector field over the phase space satisfying the Thomas–BMT equation along particle trajectories $u(s)$ (which are assumed to be integrable) and it is 1–turn periodic: $\hat{n}(u; s + C) = \hat{n}(u; s)$ where C is the circumference of the ring.

The field $\hat{n}(u; s)$ is a key object for systematizing spin dynamics in storage rings. It provides a reference direction for spin at each point in phase space and it is now called the

"invariant spin field" [2, 7, 8]. At zero orbital amplitude, i.e. on the periodic ("closed") orbit, the $\hat{n}(0; s)$ is written as $\hat{n}_0(s)$. For $e^\pm$ rings and away from spin–orbit resonances (see below), $\hat{n}$ is normally at most a few milliradians away from $\hat{n}_0$.

A central ingredient of the D–K formalism is the implicit assumption that the $e^\pm$ polarization at each point in phase space is parallel to $\hat{n}$ at that point. In the approximation that the particles have the same energies and are traveling in the same direction, the polarization of a bunch measured in a polarimeter at s is then the ensemble average

$$\vec{P}_{\text{ens,dk}}(s) = P_{\text{dk}} \langle \hat{n} \rangle_s . \tag{6}$$

In conventional situations in $e^\pm$ rings, $\langle \hat{n} \rangle_s$ is very nearly aligned along $\hat{n}_0(s)$. The *value* of the ensemble average, $P_{\text{ens,dk}}(s)$, is essentially independent of s.

Equation 5 can be viewed as having three components. The piece

$$P_{\text{bk}} = \mp \frac{8}{5\sqrt{3}} \frac{\oint ds \left\langle \frac{1}{|\rho(s)|^3} \hat{b} \cdot \hat{n} \right\rangle_s}{\oint ds \left\langle \frac{1}{|\rho(s)|^3}(1 - \frac{2}{9}(\hat{n} \cdot \hat{s})^2) \right\rangle_s} \approx \mp \frac{8}{5\sqrt{3}} \frac{\oint ds \frac{1}{|\rho(s)|^3} \hat{b} \cdot \hat{n}_0}{\oint ds \frac{1}{|\rho(s)|^3}(1 - \frac{2}{9} n_{0s}^2)} . \tag{7}$$

gives the equilibrium polarization due to radiative spin flip. The quantity n_{0s} is the component of $\hat{n}_0$ along the closed orbit. The subscript "bk" is used here instead of "st" to reflect the fact that this is the generalization by Baier and Katkov [9, 10] of the original S–T expression to cover the case of piecewise homogeneous fields. Depolarization is then accounted for by including the term with $\frac{11}{18} \left(\frac{\partial \hat{n}}{\partial \delta} \right)^2$ in the denominator. Finally, the term with $\frac{\partial \hat{n}}{\partial \delta}$ in the numerator is the so–called kinetic polarization term. This results from the dependence of the radiation power on the initial spin direction and is not associated with spin flip. It can normally be neglected but is still of interest in rings with special layouts.

In the presence of radiative depolarization the rate in Eq. 2 must be replaced by

$$\tau_{\text{dk}}^{-1} = \frac{5\sqrt{3}}{8} \frac{r_{\text{e}} \gamma^5 \hbar}{m_{\text{e}}} \frac{1}{C} \oint ds \left\langle \frac{1 - \frac{2}{9}(\hat{n} \cdot \hat{s})^2 + \frac{11}{18} \left(\frac{\partial \hat{n}}{\partial \delta} \right)^2}{|\rho(s)|^3} \right\rangle_s . \tag{8}$$

This can be written in terms of the spin–flip polarization rate, τ_{bk}^{-1}, and the depolarization rate, τ_{dep}^{-1}, as:

$$\frac{1}{\tau_{\text{dk}}} = \frac{1}{\tau_{\text{bk}}} + \frac{1}{\tau_{\text{dep}}} , \tag{9}$$

where

$$\tau_{\text{dep}}^{-1} = \frac{5\sqrt{3}}{8} \frac{r_{\text{e}} \gamma^5 \hbar}{m_{\text{e}}} \frac{1}{C} \oint ds \left\langle \frac{\frac{11}{18} \left(\frac{\partial \hat{n}}{\partial \delta} \right)^2}{|\rho(s)|^3} \right\rangle_s \tag{10}$$

and

$$\tau_{\text{bk}}^{-1} = \frac{5\sqrt{3}}{8} \frac{r_{\text{e}} \gamma^5 \hbar}{m_{\text{e}}} \frac{1}{C} \oint ds \left\langle \frac{1 - \frac{2}{9}(\hat{n} \cdot \hat{s})^2}{|\rho(s)|^3} \right\rangle_s . \tag{11}$$

3

The time dependence for build–up from an initial polarization P_0 to equilibrium is

$$P(t) \;=\; P_{\mathrm{ens,dk}}\left[1 - e^{-t/\tau_{\mathrm{dk}}}\right] + P_0 e^{-t/\tau_{\mathrm{dk}}} \;. \tag{12}$$

In perfectly aligned $e^{\pm}$ storage rings containing just horizontal bends, quadrupoles and accelerating cavities, there is no vertical betatron motion and $\hat{n}_0(s)$ is vertical. Since the spins do not "see" radial quadrupole fields and since the electric fields in the cavities are essentially parallel to the particle motion, $\hat{n}$ is vertical, parallel to the guide fields and to $\hat{n}_0(s)$ at all u and s. Then the derivative $\frac{\partial \hat{n}}{\partial \delta}$ vanishes and there is no depolarization. However, real rings have misalignments. Then there is vertical betatron motion so that the spins also see radial fields which tilt them from the vertical. Moreover, $\hat{n}_0(s)$ is also tilted and the spins can couple to vertical quadrupole fields too. As a result $\hat{n}$ becomes dependent on u and "fans out" away from $\hat{n}_0(s)$ by an amount which usually increases with the orbit amplitudes. Then in general $\frac{\partial \hat{n}}{\partial \delta}$ no longer vanishes in the dipoles (where $1/|\rho(s)|^3$ is large) and depolarization occurs. In the presence of skew quadrupoles and solenoids and in particular in the presence of spin rotators, $\frac{\partial \hat{n}}{\partial \delta}$ can be non–zero in dipoles even with perfect alignment. The deviation of $\hat{n}$ from $\hat{n}_0(s)$ and the depolarization tend to be particularly large near to the spin–orbit resonance condition

$$\nu_{\mathrm{spin}} \;=\; k_0 + k_I \nu_I + k_{II} \nu_{II} + k_{III} \nu_{III} \;. \tag{13}$$

Here $k_0, k_I, k_{II}, k_{III}$ are integers, $\nu_I, \nu_{II}, \nu_{III}$ are the three tunes of the synchrobetatron motion and ν_{spin} is the spin tune on the closed orbit, i.e. the number of precessions around $\hat{n}_0(s)$ per turn, made by a spin on the closed orbit [1]. In the special case, or in the approximation, of no synchrobetatron coupling one can make the associations: $I \to x$, $II \to y$ and $III \to s$, where, here, the subscript s labels the synchrotron mode. In a simple flat ring with no closed orbit distortion, $\nu_{\mathrm{spin}} = a\gamma_0$ where γ_0 is the Lorentz factor for the nominal beam energy. For $e^{\pm}$, $a\gamma_0$ increments by 1 for every 441 MeV increase in beam energy. In the presence of misalignments and special elements like rotators, ν_{spin} is usually still approximately proportional to the beam energy. Thus an energy scan will show peaks in τ_{dep}^{-1} and dips in $P_{\mathrm{ens,dk}}(s)$, namely at the resonances. Examples can be seen in figure 3 below. The resonance condition expresses the fact that the disturbance to spins is greatest when the $|\vec{\Omega}(u;s) - \vec{\Omega}(0;s)|$ along an orbit is coherent ("in step") with the natural spin precession. The quantity $(|k_I| + |k_{II}| + |k_{III}|)$ is called the order of the resonance. Usually, the strongest resonances are those for which $|k_I| + |k_{II}| + |k_{III}| = 1$, i.e. the first order resonances. The next strongest are usually the so–called *"synchrotron sideband resonances"* of parent first order resonances, i.e. resonances for which $\nu_{\mathrm{spin}} = k_0 \pm \nu_{I,II,III} + \tilde{k}_{III} \nu_{III}$ where $\tilde{k}_{III}$ is an integer and mode III is associated with synchrotron motion. All resonances are due to the non–commutation of successive spin rotations in 3–D and they therefore occur even with purely linear orbital motion.

We now list some keys points.

- The approximation on the r.h.s. of Eq. 7 makes it clear that if there are dipole magnets with fields not parallel to $\hat{n}_0$, as is the case, for example, when spin rotators are used,

---

[1] In fact the resonance condition should be more precisely expressed in terms of the so–called amplitude dependent spin tune [2, 7, 8]. But for typical $e^{\pm}$ rings, the amplitude dependent spin tune differs only insignificantly from ν_{spin}.

then P_{bk} can be lower than the 92.4% achievable in the case of a simple ring with no solenoids and where all dipole fields and $\hat{n}_0(s)$ are vertical.

- If, as is usual, the kinetic polarization term makes just a small contribution, the above formulae can be combined to give

$$P_{\text{ens,dk}} \quad \approx \quad P_{\text{bk}} \frac{\tau_{\text{dk}}}{\tau_{\text{bk}}} \ . \tag{14}$$

From Eq. 9 it is clear that $\tau_{\text{dk}} \leq \tau_{\text{bk}}$.

- The underlying rate of polarization due to the S–T effect, τ_{bk}^{-1}, increases with the fifth power of the energy and decreases with the third power of the bending radii.

- It can be shown that as a general rule the "normalized" strength of the depolarization, $\tau_{\text{dep}}^{-1}/\tau_{\text{bk}}^{-1}$, increases with beam energy according to a tune dependent polynomial in even powers of the beam energy.

Pre–polarization

Instead of relying on self polarization, for e^- one can inject a pre–polarized beam. The polarized e^- are supplied by a gallium arsenide source and then accelerated in a linear accelerator to full energy. Gallium arsenide sources can provide polarizations of 80%. Acceleration in a recirculating device is also possible provided measures are taken to avoid depolarization when accelerating through resonances. The CEBAF machine at the Thomas Jefferson National Accelerator Facility is an example of such a device. These matters are discussed in other sections. It would be necessary to inject the pre-polarized e^- at full energy since it is unlikely that the polarization would survive resonance crossing during acceleration in the ring itself.

Since no simple polarized sources exist for e^+, a pre–polarized e^+ beam would have to be polarized by the S–T effect in a dedicated preceding ring.

To avoid an immediate loss of polarization in the recipient ring, the polarization vector should lie along the $\hat{n}_0$ vector at the injection point. In that case the subsequent time dependence is given by Eq. 12. Note that if the injected polarization is higher than the $P_{\text{ens,dk}}$, the polarization will *fall* to this value with the characteristic time τ_{dk}. Furthermore, if the injected polarization has the "wrong" sign, the S–T effect will drive the polarization through zero and into the natural direction. Again, the characteristic time will be τ_{dk} and the final value will be $P_{\text{ens,dk}}$. Injecting a pre–polarized beam is the only solution if the required energy of the stored beam is so low that τ_{bk} is impractically large. It is also useful if the lifetime of the stored beam is small: full polarization is immediately available while the luminosity is still high.

Software

There are two classes of computer algorithm for estimating the equilibrium polarization in real $e^{\pm}$ rings:

(i) Methods based on evaluating $\hat{n}$ and $(\frac{\partial \hat{n}}{\partial \delta})^2$ in the D–K formula given the ring layout and magnet strengths; and

(ii) a more pragmatic approach in which particles and their spins are tracked while photon emission is simulated approximately within a Monte–Carlo framework and τ_{dep} is "measured". Eqs. 9 and 14 then provide an estimate of τ_{dk} and the equilibrium polarization. The programs SITROS [11] and SLICKTRACK [12] exemplify this approach.

The class (i) algorithms are further divided according to the degree of linearization of the spin and orbital motion:

(ia) The SLIM family (SLIM [13, 14], SLICK [15], SITF [11]) and SOM [16] and ASPIRRIN [17]. The last two utilize approximate versions of the *"betatron–dispersion"* formalism [1] and all are based on a linearization of the orbital and spin motion. For spin, the linearization involves assuming that the angle between $\hat{n}$ and $\hat{n}_0$ is small at all positions in phase space so that $\hat{n}$ can be approximated by the form $\hat{n}(u; s) \approx \hat{n}_0(s) + \alpha(u; s)\hat{m}(s) + \beta(u; s)\hat{l}(s)$. The unit vectors $\hat{m}$ and $\hat{l}$ are 1–turn periodic and chosen so that the set $\{\hat{n}_0, \hat{m}, \hat{l}\}$ is orthonormal. It is assumed that $\sqrt{\alpha^2 + \beta^2} \ll 1$. This approximation reveals just the first order spin–orbit resonances and it breaks down when $\sqrt{\alpha^2 + \beta^2}$ becomes large very close to these resonances.

(ib) SMILE [6]: Linearized orbital motion but "full" spin motion using a high order perturbation theory.

(ic) SODOM [18]: Linearized orbital motion but full spin motion expressed by a Fourier expansion.

Note that the precise evaluation of $\hat{n}$ and $(\frac{\partial \hat{n}}{\partial \delta})^2$ requires calculating beyond the linear approximation. Then large amounts of computer power are needed, especially if a large number of resonances must be taken into account. Thus the calculations presented here are based on a class (ia) algorithm, in particular that in SLICK. This executes very quickly and it furnishes valuable first impressions, even though it can only exhibit the first order resonances. At a later stage results from SLICKTRACK based on a class (ii) algorithm and full spin motion will be available. Then the influence of higher order resonances will be seen. This kind of algorithm also allows the effect of non–linear orbital motion and the beam–beam interaction to be studied. The class (ii) algorithm is mathematically much simpler than the class (i) algorithm but it still requires a large amount of computing power for the simulation for long enough of the motion of enough particles and their spins.

Spin rotators

The eRHIC project, like all analogous projects involving spin, needs longitudinal polarization at the interaction point. However, if the S–T effect is to be the means of making and maintaining the polarization, then as is clear from Eq. 7, $\hat{n}_0$ must be close to vertical in most of the dipoles. We have seen at Eq. 6 that the polarization is essentially parallel to $\hat{n}_0$. So to get longitudinal polarization at a detector, it must be arranged that $\hat{n}_0$ is longitudinal at the detector but vertical in the rest of the ring. This can be achieved with magnet systems

called spin rotators which rotate $\hat{n}_0$ from vertical to longitudinal on one side of the detector and back to vertical again on the other side. Eq. 7 shows that P_{bk} essentially scales with the cosine of the angle of tilt of $\hat{n}_0$ from the vertical in the arc dipoles. Thus a rotation error resulting in a tilt of $\hat{n}_0$ of even a few degrees would not reduce P_{bk} by too much. However, as was mentioned above, a tilt of $\hat{n}_0$ in the arcs can lead to depolarization and calculations show that tilts of more than about a degree produce significant depolarization. Thus well tuned rotators are essential for maintaining polarization even if the beam is pre–polarized before injection.

Suppression of depolarization – spin matching

Although the S–T effect offers a convenient way to obtain stored high energy $e^{\pm}$ beams, it is only useful in practice if there is not too much depolarization. Depolarization can also limit the usefulness of beams pre–polarized before injection: τ_{dk} must be large enough to ensure that the large injected polarization survives until it is safe to switch on the sensitive parts of the detector after injection and survives long enough for collecting enough data in the detector. Depolarization can be significant if the ring is misaligned, if it contains spin rotators or if it contains uncompensated solenoids or skew quadrupoles. Then if $P_{\mathrm{ens,dk}}$ and/or τ_{dk} are too small, the layout and the optic must be adjusted so that $(\frac{\partial \hat{n}}{\partial \delta})^2$ is small where $1/|\rho(s)|^3$ is large. So far it is only possible to do this within the linear approximation for spin motion. This technique is called *"linear spin matching"* and when successful, as for example at HERA [19], it immediately reduces the strengths of the first order spin–orbit resonances. Spin matching requires two steps: *"strong synchrobeta spin matching"* is applied to the optics and layout of the perfectly aligned ring and then *"harmonic closed orbit spin matching"* is applied to soften the effects of misalignments. This latter technique aims to adjust the closed orbit so as to reduce the tilt of $\hat{n}_0$ from the vertical in the arcs. Since the misalignments can vary in time and are usually not sufficiently well known, the adjustments are applied empirically while the polarization is being measured.

Spin matching must be approached on a case by case basis. An overview can be found in [1]. Spin matching for eRHIC will discussed later.

Higher order resonances

Even if the beam energy is chosen so that first order resonances are avoided and in linear approximation $P_{\mathrm{ens,dk}}$ and/or τ_{dk} are expected to be large, it can happen that that beam energy corresponds to a higher order resonance. In practice the most intrusive higher order resonances are those for which $\nu_{\mathrm{spin}} = k_0 \pm \nu_k + \tilde{k}_s \nu_s$ ($k \equiv I, II$ or III). These synchrotron sideband resonances of the first order parent resonances are due to modulation by energy oscillations of the instantaneous rate of spin precession around $\hat{n}_0$. The depolarization rates associated with sidebands of isolated parent resonances ($\nu_{\mathrm{spin}} = k_0 \pm \nu_k$) are related to the depolarization rates for the parent resonances. For example, if the beam energy is such that the system is near to a dominant ν_y resonance we can approximate τ_{dep}^{-1} in the form

$$\tau_{\mathrm{dep}}^{-1} \propto \frac{A_y}{\left(\nu_{\mathrm{spin}} - k_0 \pm \nu_y\right)^2} \ . \tag{15}$$

7

This becomes

$$\tau_{\text{dep}}^{-1} \propto \sum_{\tilde{k}_s=-\infty}^{\infty} \frac{A_y\, B_y(\zeta; \tilde{k}_s)}{\left(\nu_{\text{spin}} - k_0 \pm \nu_y \pm \tilde{k}_s\, \nu_s\right)^2}$$

if the synchrotron sidebands are included. The quantity A_y depends on the beam energy and the optics and is reduced by spin matching. The proportionality constants $B_y(\zeta; \tilde{k}_s)$ are called *enhancement factors*, and they contain modified Bessel functions $I_{|\tilde{k}_s|}(\zeta)$ and $I_{|\tilde{k}_s|+1}(\zeta)$ which depend on the *modulation index* $\zeta = (a\gamma_0\, \sigma_\delta/\nu_s)^2$. More formulae can be found in [20].

Thus the effects of synchrotron sideband resonances can be reduced by doing the spin matches described above. Note that these formulae are just meant as a guide since they are approximate and explicitly neglect interference between the first order parent resonances. To get a complete impression, the Monte–Carlo simulation mentioned earlier must be used. The sideband strengths generally increase with the energy spread and the beam energy.

2.4.6 2 Spin polarization in eRHIC

Choice of rotators

For rings like eRHIC two kinds of rotator can be considered: *"solenoid rotators"* and *"dipole rotators"*. The current design employs solenoid rotators. Dipole rotators will be mentioned later.

Various layouts of rotators involving solenoids can be conceived [21, 22, 23]. The layout considered for eRHIC is sketched in figure 1. The vertical $\hat{n}_0$ in the arc is rotated by 45 degrees towards the horizontal by the longitudinal field of the first solenoid. A second solenoid completes the rotation into the horizontal plane. The vector $\hat{n}_0$ is then rotated from the radial direction towards the longitudinal direction by a string of horizontally bending dipoles. The orbital deflection required is $90/a\gamma_0$ degrees.

After the interaction point a string of dipoles of reverse polarity rotates $\hat{n}_0$ back to the radial direction and two solenoids with polarity opposite to that of the first two rotate $\hat{n}_0$ back to the vertical. Then $\hat{n}_0$ is vertical in the arcs at all beam energies. If a solenoid rotates $\hat{n}_0$ by 45 degrees, then for $e^{\pm}$ the plane of the transverse particle distribution is rotated by about 22.5 degrees so that the rotator can generate strong transverse orbital coupling. However, this coupling is eliminated by correctly choosing the strengths and positions of quadrupoles placed within the first pair of solenoids and within the last pair (figure 1). The orbital motion between the first and second pair of solenoids is uncoupled and the quadrupole strengths in that region can be chosen as required.

Some advantages and disadvantages of solenoid rotators are:

Advantages:

- The arrangement is compact.

- In contrast to the dipole rotators discussed later, no vertical orbit excursion is needed.
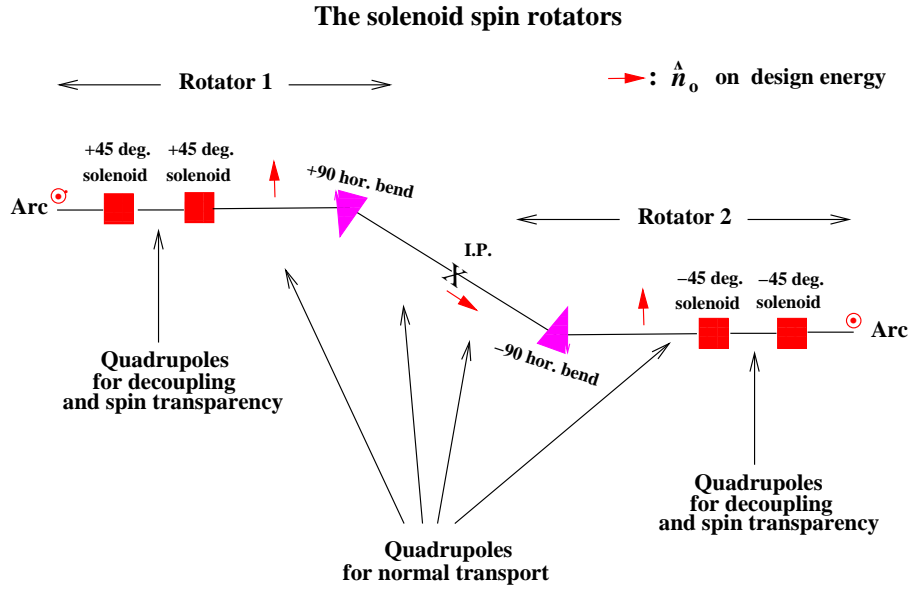
8

The solenoid spin rotators

Figure 1: The schematic layout of the solenoid rotators. Only the positions and functions of the key elements are shown. Each rotator consists of two solenoids and horizontal bend magnets, to rotate $\hat{n}_0$ into (or out of) the longitudinal direction. Quadrupoles tuned to ensure transverse decoupling and spin transparency w.r.t. x and x' are placed between each solenoid in each rotator. Antisymmetric horizontal bends very near the interaction point are not shown.

- The sign of the longitudinal component of the equilibrium polarization at the interaction point can be reversed by simply changing the polarities of all the solenoids.

Disadvantages:

- The polarization is longitudinal at just one beam energy and that energy is defined by the field integrals of the horizontally bending dipoles on each side of the interaction point. Any remedy for this restriction would require elaborate engineering involving moving the solenoids. However, if it is planned to run eRHIC just around 10 GeV, say in the range 9.69 to 10.13 GeV ($\Longrightarrow 22 \lesssim a\gamma_0 \lesssim 23$), $\hat{n}_0$ will always be within about 2 degrees of the beam direction.

- By the Thomas–BMT equation the rate of spin precession in a solenoid is inversely proportional to the beam energy. So solenoid spin rotators are only practical at low energy. At 10 GeV each solenoid needs a field integral of about 26.7 Tm and must therefore be superconducting.

- The solenoids cause transverse coupling which must be eliminated by introducing special quadrupole arrangements. Solenoid spin rotators are also not automatically spin transparent (see below).

A corresponding list of advantages and disadvantages for dipole rotators is given later.

The horizontal dispersion should be zero on entry to the first solenoid and at the exit from the last and the horizontal dispersion is set to zero at the interaction point.

Spin matching with the solenoid rotators

To explain the spin matching conditions needed when the solenoid rotators are used we begin by considering a flat, perfectly aligned ring without the rotators, the detector and the oncoming proton beam. In this case there is no vertical closed orbit distortion and the radiation damping together with the absence of vertical dispersion ensure that the beam has essentially zero thickness. Then as explained earlier, $\hat{n}_0$ is vertical and $\hat{n}(u; s)$ is vertical at all u and all s. The derivative $\frac{\partial \hat{n}}{\partial \delta}$ is then zero and there is no depolarization.

However, the solenoids have radial end fields which can tilt spins from the vertical and the longitudinal fields tilt spins step–wise into and out of the horizontal plane so that they then precess in the vertical fields of the quadrupoles inside and between the rotators. Inside a rotator, they also precess in the radial quadrupole fields at the non-zero y induced by the first solenoid of a pair. Moreover, the total angle of rotation in the two solenoids of a rotator is ± 90 degrees only at $\delta = 0$. Since $\hat{n}(u; s)$ is a functional of the geometry and optics of the ring we see that unless special measures are taken, the solenoid rotators will cause $\hat{n}$ to depend on u and s. Then $\frac{\partial \hat{n}}{\partial \delta}$ will not vanish in the dipoles in the arcs and there will be depolarization.

The solution is to make the section from the entrance of the first rotator to the exit of the second rotator *"spin transparent"*, i.e. to choose the strengths and positions of quadrupoles and dipoles in this section so that in the approximation of linearized spin motion, the total rotation of a spin around and w.r.t. $\hat{n}_0$ vanishes for a spin beginning with arbitrary u and traversing this section. We have already mentioned that we eliminate the generation of transverse coupling by the solenoids with the aid of quadrupoles placed within the solenoid pairs. It then turns out that spin transparency w.r.t. x and x' can be arranged in addition, and in a straightforward way, by setting these quadrupoles such that the 4×4 transfer matrix for the transverse motion through a pair has the form [21]

$$\begin{pmatrix} 0 & -2r & 0 & 0 \\ 1/2r & 0 & 0 & 0 \\ 0 & 0 & 0 & 2r \\ 0 & 0 & -1/2r & 0 \end{pmatrix} \tag{16}$$

where r is the radius of orbit curvature in the longitudinal field of a solenoid and where the elimination of coupling is explicit. The optic between the rotators should be uncoupled. Since the integral of the solenoid fields vanishes for the whole region, at first order there is no net spin perturbation resulting from non–zero δ in the solenoids. Moreover, the constraints on the horizontal dispersion and the layout of the dipoles around the interaction point ensure that the change in direction of the horizontal dispersion, due to quadrupole fields, vanishes for the stretch between the second and third solenoids. Thus there is transparency w.r.t. longitudinal motion too [1]. Providing that the constraints on the dispersion are satisfied, the optic between the second and third solenoids can be chosen at will independently of the need to ensure spin transparency, once the matrices for the rotators have the form just given. So far it has not been necessary to consider spin transparency w.r.t. y and y' since in the perfectly aligned ring and with transverse coupling restricted to the rotators themselves, synchrotron radiation in the arcs does not excite vertical motion. Then $y = 0$ and $y' = 0$ on entering a rotator from the arc. With these conditions it is easy to show that with linearized

spin motion and perfect alignment, $\frac{\partial \hat{n}}{\partial \delta}$ indeed vanishes at all dipoles in the arcs [1]. We say that the ring is spin matched at each dipole in the arcs.

Thus although an isolated solenoid is not spin transparent, we have a very elegant way to ensure sufficient overall spin transparency of the whole rotator insertion. Moreover, from the above discussion about the requirements for the optic in the stretch between the second and third solenoids, it is clear that the depolarizing effects from beam-beam forces should be suppressed. The same probably applies to the detector field if it can be prevented from generating coupling. These count among the advantages of such solenoid spin rotators.

Note that our spin matching conditions do not ensure that $\frac{\partial \hat{n}}{\partial \delta}$ vanishes in the dipoles between the rotators. Moreover, since $\hat{n}_0$ is horizontal in the vertical fields of those dipoles, Eq. 7 implies that P_{bk} can be lower than 92.4%. However, this lowering of P_{bk} can be limited by making the dipoles long enough to ensure that their $\int ds/|\rho(s)|^3$ is small compared to that in the arcs. We return to these two points below.

Calculations of the $e^\pm$ polarization in eRHIC

Following this lengthy introduction we now present first calculations of the polarization. The calculations are carried out with the thick lens code SLICK. This accounts for just the first order spin–orbit resonances. No account is taken of the magnetic field of the detector and there is no beam–beam force from oncoming protons. The horizontal and vertical betatron phase advances in the arc cells are 72 and 60 degrees respectively and the fractional parts of the betatron tunes are $[\nu_x] = 0.105$ and $[\nu_y] = 0.146$. The synchrotron tune, ν_s, is 0.044. SLICK automatically produces the correct transverse and longitudinal emittances.
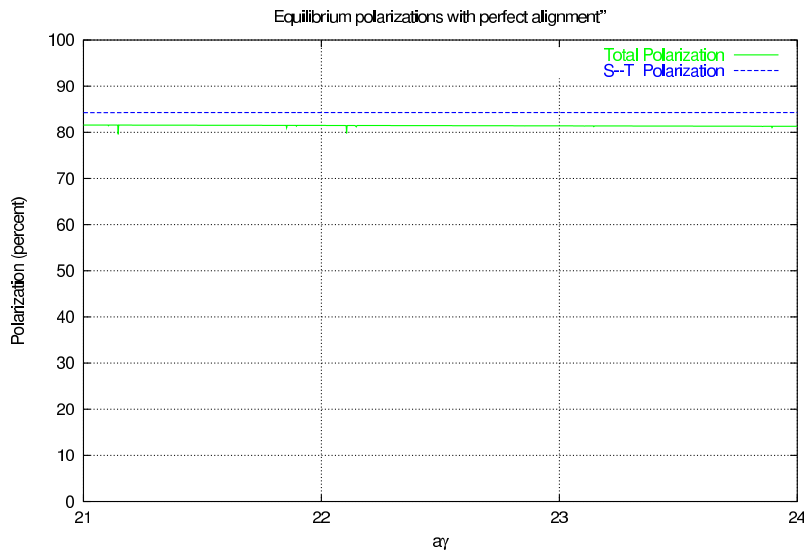

Figure 2: The polarizations P_{bk} and P_{dk} for a perfectly aligned ring containing a spin transparent pair of solenoid spin rotators.

Figure 2 shows the equilibrium polarization for the perfectly aligned ring in the range 9.25 to 10.58 GeV. With these rotators the spin tune, ν_{spin}, on the design orbit is $a\gamma_0$. Thus

11

this energy range corresponds to $21 \leq \nu_{\mathrm{spin}} \leq 24$, i.e. it spans three full integers. It is seen that P_{bk} (labeled as S–T Polarization) is almost independent of energy at about 84.3%. It is below 92.4% because $\hat{n}_0$ is perpendicular to the fields in the dipoles around the interaction point. Recall Eq. 7. The actual polarization, P_{dk} (labeled as Total Polarization), is about 81.7%. The additional decrease of about 2.6% is due to the depolarization caused by the non–zero $(\frac{\partial \hat{n}}{\partial \delta})^2$ in those dipoles. It is interesting that although there is some depolarization, this depolarization shows no resonant structure. This can be understood in terms of some 1–turn integrals appearing in the calculation of $\frac{\partial \hat{n}}{\partial \delta}$ [1]. When these integrals are evaluated starting somewhere in the arc, they are zero because of the spin matching. At resonance these integrals are independent of the starting point. Then they are zero starting at the dipoles around the interaction point and the factors A_x and A_s analogous to the A_y of Eq. 15 vanish at resonance.
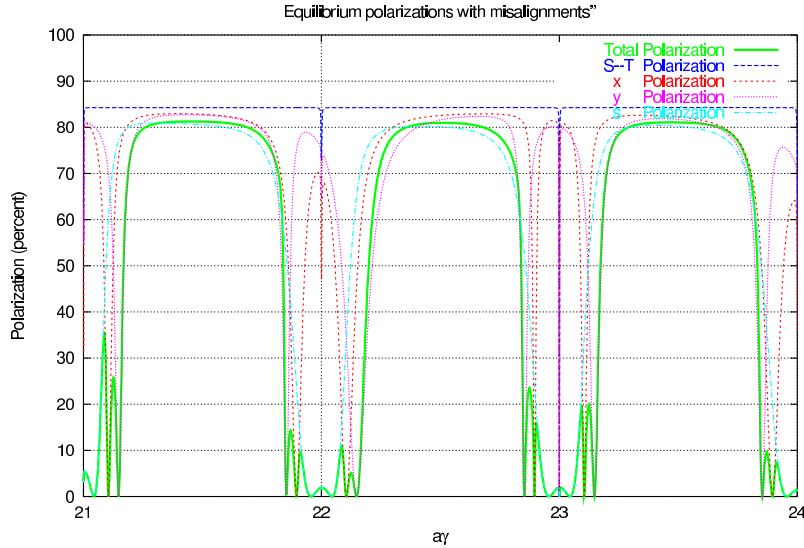

Figure 3: The polarizations P_{bk} and P_{dk} and the polarizations associated with each of the three orbital modes when realistic imperfections are applied and the orbit is subsequently corrected.

As stated earlier, misalignments can lead to depolarization. In fact experience shows that misalignments can be very dangerous and that care should be invested in the alignment of the ring and measurement of the orbit. Care is also needed for realistic simulations. Figure 3 shows results of calculations of equilibrium polarizations with SLICK for typical realistic misalignments and after orbit correction. Figure 4 shows the corresponding τ_{bk} and τ_{dk}. The τ_{bk} exhibits the characteristic γ_0^{-5} dependence. At 9.91 GeV ($a\gamma = 22.5$) τ_{bk} and τ_{dk} are about 21 and 20 minutes respectively. At 5 GeV τ_{bk} would be about 11 hours. In that case self polarization would not be practical and a pre-polarised beam would be needed. Otherwise the average $1/|\rho(s)|^3$ would have to be greatly increased [24].

The misalignments include vertical shifts and roll on the quadrupoles, roll on the dipoles and errors on the beam position monitors. Scale errors on the quadruple strengths are also included. A monitor and horizontal and vertical correction coils are assigned to each
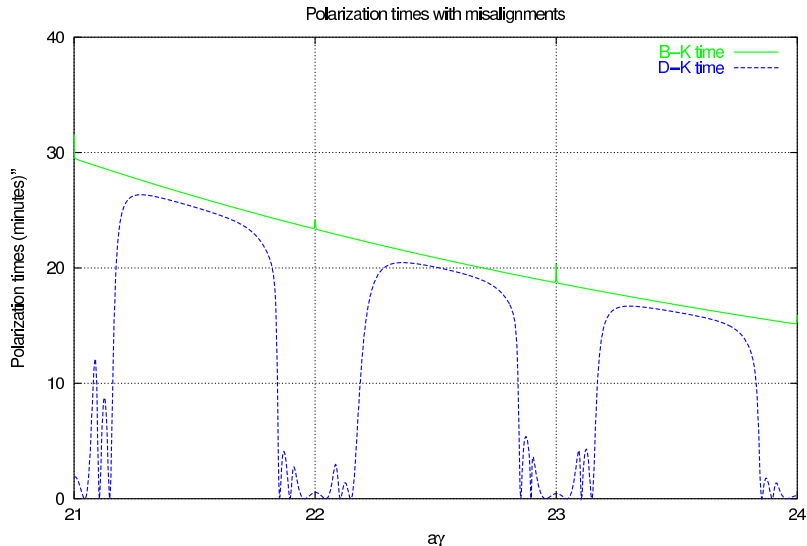
12

Figure 4: The characteristic times τ_{bk} and τ_{dk} (minutes) for the simulation in figure 3.

quadrupole. Figure 3 shows five curves: P_{bk} (labeled as S–T Polarization), P_{dk} (bold, labeled as Total Polarization), and each of the polarizations that would be reached if just one orbital mode were excited. The first order resonances are clearly visible and can easily be identified using the known values of $[\nu_x]$, $[\nu_y]$ and ν_s. Note that the ν_s resonances are so strong that they overlap around integer values of ν_{spin} [2]. In this simulation the peak values of P_{dk} are about 81.5% and occur near half integer values of ν_{spin}. This is characteristic behavior and shows that the beam energy should be set for such values. It is also clear, as usual, that the fractional parts of the orbital tunes should be as far away from $1/2$ as is practical to "leave space" around half integer spin tune. It might then be the case that the synchrotron sideband resonances are weak at the recommended energies. This conjecture will be checked at a later stage using a class (ii) simulation. Different choices of the random numbers specifying the imperfections lead to curves which differ in detail from those in figures 3 and 4. However, the curves remain qualitatively similar. Before orbit correction the polarization is very small.

In this simulation the tilt of $\hat{n}_0$ in the arcs is about 2.5 milliradians at the maxima of P_{dk}. The r.m.s. vertical deviation of the closed orbit from the design machine plane is 0.034 mm after the orbit correction mentioned above. The maximum deviation is 0.18 mm. Such small residual closed orbit deviations might look optimistic but realistic misalignments have been assumed and these small residuals arise naturally with the orbit correction algorithm used here. Moreover, the problem of obtaining very small residual closed orbit deviations has been conquered for modern synchrotron radiation sources. Note that the closed orbit deviations remain small and the peak polarizations remain high even if a random sample of 20% of the monitors is taken out of service. In any case the sensitivity of the polarization

---

[2]But for this first order calculation τ_{dk} does *not* vanish at integer values of ν_{spin}: there are no "integer resonances" in τ_{dk}^{-1}. However, the S–T effect becomes very weak at integer values of ν_{spin} as $\hat{n}_0$ tilts strongly from the vertical in the arcs.

13

to such small deviations shows that *it would be a false economy to skimp on good alignment of the ring, on the provision of correction magnets and on the precision of the beam position monitors.* One should also avoid stray fields from the proton ring and magnetic material in the beam pipe. Experience at HERA [19] supports this view.

Since the tilt of $\hat{n}_0$ is already small, harmonic closed orbit spin matching has not yet been applied. Perhaps with good enough alignment and corrections it would not be needed.

The calculations carried out so far show that with linearized spin motion and in the absence of detector fields and beam–beam forces, both high equilibrium polarizations and reasonable τ_{dk} can be achieved around 10 GeV. Then operation with either self polarized $e^{\pm}$ or with pre-polarized e^{-} would be comfortable. For the latter it would be necessary to avoid loss of polarization during injection. Note that in contrast to the injection of polarized protons into a ring, e^{-} are subject to *stochastic* depolarization as the beam reaches equilibrium.

Although the results from linearized calculations give strong grounds for optimism, a complete picture will only emerge once full spin motion has been included as well as other effects which have been neglected so far. Some next steps in this direction are discussed below. In the meantime it is important to note that 51% longitudinal e^{+} polarization has already been achieved simultaneously at three interaction points at HERA at the almost three times higher energy of 27.5 GeV [25, 26].

To achieve high luminosity it will be necessary to mount quadrupoles inside the detector solenoid. These magnets will then be subject to large inter–magnet forces. Thus special efforts should be invested in the stability of their mounts and the monitoring of their positions so that they do not cause excessive closed orbit distortion and resultant depolarization. Use should be made of experience with HERA [25].

Some next steps

So far, it appears that with good orbit correction, harmonic closed orbit spin matching will not be needed. Nevertheless this topic still needs to be thoroughly studied.

Since there is no simple way in standard optics software to represent the effects on the trajectories and the spins of the complicated overlapping fields of solenoids and quadrupoles, special spin–orbit maps for the interaction regions should be established. The calculations with SLICK should then be repeated using the linear parts of these maps to establish whether in linear approximation these combined fields have a significant influence on the spin transparency of the rotator section and on the polarization. The methods used for HERA could be adopted here [27, 26].

The calculations with linearized spin motion do not include the effects of higher order spin–orbit resonances. Thus a next step will be to carry out class (ii) simulations with SLICKTRACK. This will, for example, give a picture of the strengths of the synchrotron sideband resonances and of whether there are advantages in choosing a special ν_s.

Even with misalignments the natural beam height will be very small. But as has been mentioned elsewhere, to reach high luminosity it will be necessary to increase the beam height. This might be achieved by, for example, running close to a transverse coupling resonance. Perhaps other methods can be found. In any case experience shows that a proper picture of the polarization for such situations will require using a class (ii) simulation.

Class (ii) simulations are also essential for understanding the full effects of beam–beam forces on the polarization and the effects of non–linear orbital motion including the motion in the complicated fields in the detector.

Class (ii) simulations will also be necessary for evaluating the behavior of the polarization of a pre–polarized beam during injection.

Spin flip

As stated earlier, with the solenoid rotators the sign of the equilibrium longitudinal polarization can be changed by reversing the polarity of the solenoids. But this cannot be done while the beam is stored. However, it might still be possible to reverse the polarization on short time scales and without dumping the beam, by using resonant spin flip driven by an external radio frequency magnetic field. Note that after a reversal the polarization would return through zero to its original orientation with the characteristic time τ_{dk}. Resonant flipping of electron spins has been demonstrated at low energy [28] but it remains to be seen whether it is practical at the much higher energy of 10 GeV where spin diffusion might limit the efficiency [29, 30]. Class (ii) simulations will also provide insights here.

2.4.6 3 Further aspects of spin rotation

Although solenoid rotators have been chosen for eRHIC, dipole rotators can be kept in reserve.

The simplest kind of dipole rotator system involves just vertical bends which generate a Z shaped modification of the design orbit in the vertical plane [31, 32]. But the design orbit is then sloped at the interaction point and the detector which are just at the midpoint of the system. To reverse the sign of the equilibrium longitudinal polarization, the polarities of the vertical bends and the vertical positions of all the magnets w.r.t. the plane of the ring must be reversed. This in turn requires very flexible bellows between magnets and a mechanical jacking system for the whole interaction region including the quadrupoles very close to the detector.

A much more practical and economical solution is to use spin rotators consisting of strings of interleaved vertical and horizontal bends arranged so that they produce interleaved horizontal and vertical closed beam bumps. Such rotators stand apart from the detector and its nearby quadrupoles. According to the Thomas–BMT equation an orbit deflection of $\delta\theta_{\mathrm{orb}}$ in a transverse magnetic field produces a spin rotation of $\delta\theta_{\mathrm{spin}} = (a\gamma+1)\delta\theta_{\mathrm{orb}}$. Then at high energy small orbit deflections lead to large spin rotations and although the combined orbit bumps close, $\hat{n}_0$ can be rotated from vertical to longitudinal before the interaction point. A second rotator returns $\hat{n}_0$ to the vertical before the next arc. This is the scheme successfully used at HERA [19].

Some advantages and disadvantages of this second kind of dipole scheme are:

Advantages:

- The design orbit is horizontal in the detector and the nearby surrounding quadrupoles.

15

- By varying the fields and the geometry of the rotators the required rotation can be achieved for a range of energies. Then the polarization can be made essentially longitudinal at any energy in the design range.

- If the rotator is sufficiently short, it need not contain quadrupoles. It is then automatically essentially spin transparent.

Disadvantages:

- As in the case of the Z bend rotator, reversal of the sign of the longitudinal polarization requires the reversal of dipole polarities, very flexible bellows and a jacking system. But in this case only the rotators themselves need jacks, not the whole interaction region. Note that such a jacking system has been in service in HERA since 1994 [19].

- At low energy the relation $\delta\theta_{\mathrm{spin}} = (a\gamma + 1)\delta\theta_{\mathrm{orb}}$ implies that sufficient spin rotation can only be achieved with vertical orbit bumps that might be impractically large.

- Dipole rotators can decrease P_{bk} since $\hat{n}_0$ is not parallel to the field in most of the magnets. The decrease is most marked if the magnets are short ($\Longrightarrow 1/|\rho(s)|^3$ large) in order to save space.

- The generation of vertical emittance in the vertical bends can require strong vertical betatron spin matching [1].

Dipole rotators are best suited for high energy. But it is likely that for energies around 10 GeV or above, a dipole rotator with a tolerable vertical closed orbit excursion could be designed for eRHIC.

If these dipole rotators contain no quadrupoles, spin matching involves making the straight sections between the rotators spin transparent for all three modes of motion and involves making the arcs between the rotators spin transparent for vertical motion [1, 19, 27].

References

[1] D.P. Barber, G. Ripken, Handbook of Accelerator Physics and Engineering, Eds. A.W. Chao and M. Tigner, World Scientific, 2nd edition (2002).

[2] Articles by D.P. Barber (some with co–authors), in proceedings of ICFA workshop "Quantum Aspects of Beam Physics", Monterey, U.S.A., 1998, World Scientific (1999). Also as DESY Report 98–96 and at the e–print archive: physics/9901038 – physics/9901044.

[3] A.A. Sokolov, I.M. Ternov, Sov. Phys. Dokl. 8(12) (1964) 1203.

[4] J.D. Jackson, "Classical Electrodynamics", 3rd edition, Wiley (1998).

[5] Ya.S. Derbenev, A.M. Kondratenko, Sov. Phys. JETP. 37 (1973) 968.

[6] S.R. Mane, Phys. Rev. A36 (1987) 105–130.

[7] G.H. Hoffstätter, M. Vogt, D.P. Barber, Phys. Rev. ST Accel. Beams 11 (2) 114001 (1999).

[8] D.P. Barber, G.H. Hoffstätter, M. Vogt, Proc. 14th Int. Spin Physics Symp., AIP Proc. 570 (2001).

[9] V.N. Baier, V.M. Katkov, Sov. Phys. JETP. 25 (1967) 944.

[10] V.N. Baier, V.M. Katkov, V.M. Strakhovenko, Sov. Phys. JETP. 31 (1970) 908.

[11] J. Kewisch et al., Phys.Rev.Lett. 62(4) (1989) 419. The program SITF is part of the SITROS package.

[12] D.P. Barber. SLICKTRACK is the version of SLICK [15] which includes Monte–Carlo spin–orbit tracking.

[13] A.W. Chao, Nucl.Inst.Meth. 180 (1981) 29.

[14] A.W. Chao, AIP Proc. 87 (1981) 395.

[15] SLICK is a thick lens version of SLIM by D.P. Barber. Private notes (1982).

[16] K. Yokoya, User's manual of **SOM**: Spin–Orbit Matching (1996).

[17] C.W. de Jager, V. Ptitsin, Yu.M. Shatunov, Proc. 12th Int. Symp. High Energy Spin Physics, World Scientific (1997).

[18] K. Yokoya, KEK Report 92-6 (1992).
K. Yokoya, DESY Report 99–006 (1999)
and at the e–print archive: physics/9902068.

[19] D.P. Barber et al., Phys. Lett. 343B (1995) 436.

[20] S.R. Mane, Nucl.Inst.Meth. A292 (1990) 52.
S.R. Mane, Nucl.Inst.Meth. A321 (1992) 21.

[21] A.A. Zholents, V.N. Litvinenko, BINP (Novosibirsk) Preprint 81–80 (1981). English translation: DESY Report L–Trans 289 (1984).

[22] D.P. Barber et al., DESY Report 82–76 (1982). Note that in that paper, the symbol $\vec{n}$ should be replaced with $\vec{n}_0$ to correspond with modern notation.

[23] D.P. Barber et al., Particle Accelerators 17 (1985) 243. Note that in that paper, the symbol $\vec{n}$ should be replaced with $\vec{n}_0$ to correspond with modern notation.

[24] V. Ptitsyn et al., Proc. 2003 IEEE Particle Accelerator Conference (PAC2003), Portland, U.S.A., (2003).

[25] F. Willeke et al., Proc. 2003 IEEE Particle Accelerator Conference (PAC2003), Portland, U.S.A., (2003).

[26] D.P. Barber, E. Gianfelice-Wendt, M. Berglund, Physics World, July 2003.

[27] G.Z.M. Berglund, Ph.D. thesis, DESY-THESIS-2001-044 (2001).

[28] V.S. Morozov et al., Phys. Rev. ST Accel. Beams 4 104002 (2001).

[29] D.P. Barber et al., Proc. 11th Int. Symp. High Energy Spin Physics,AIP Proc. 343 (1995).

[30] K. Heinemann, DESY Report 97–166 (1997) and at the e–print archive: physics/9709025.

[31] R. Schwitters, B.Richter, SLAC PEP Note 87 (1974).

[32] J. Buon, Nucl.Inst.Meth. A275 (1989) 226.